Journal of Thermal Analysis and Calorimetry, Vol. 80 (2005) 775–780

NOVEL INSTRUMENT FOR HIGH TEMPERATURE THERMOGRAVIMETRIC MEASUREMENTS IN HIGH WATER VAPOUR CONTENTS

L. Mikkelsen[1], *M. Solvang*[1*], *P. H. Larsen*[1] *and J. Blumm*[2]

[1]Materials Research Department, Risø National Laboratory, 4000 Roskilde, Denmark
[2]Netzsch Gerätebau GmbH, 95100 Selb, Germany

A novel instrument for high temperature thermogravimetric measurements in atmospheres containing high water vapour contents was developed in a collaboration between Netzsch and Risø National Laboratory. The development of the instrument was initiated to facilitate the investigation of high temperature corrosion of steels in humidified atmospheres. The instrument consists of a standard thermal analyser unit, including a new water vapour furnace, balance and sample carrier. The design of the instrument is discussed and thermogravimetric measurements on a $Fe_{78}Cr_{22}$ steel are presented.

Keywords: *corrosion, thermogravimetry, water vapour*

Introduction

A number of materials are investigated for service under extreme atmospheres at elevated temperatures. An example is FeCr based alloys that are developed as interconnect materials for use in solid oxide fuel cell stacks (SOFC) [1]. In a SOFC stack the interconnect material experiences air (possibly humidified) on the cathode side and strongly reducing atmospheres containing high water vapour concentrations (>90% H_2O) on the anode side at temperatures in the range of 700–950°C [2]. Corrosion studies under realistic conditions are a prerequisite for the development of long-term stable materials and components. The processes occurring during high temperature oxidation are dynamic, so in situ measurements are widely used to obtain information concerning the oxidation mechanisms. The most common technique to obtain in situ measurements of oxidation is by thermogravimetry (TG). This technique makes it possible to follow the kinetics of high temperature corrosion in situ [3]. Thermogravimetric analysis under high water vapour concentrations is, however, not feasible using commercially available standard equipments due to condensation of water vapour in the instrument.

Netzsch Gerätebau GmbH and Risø National Laboratory have in collaboration developed and tested a water vapour furnace for a standard Netzsch simultaneous thermal analyser.

The layout of the instrument is described in the following along with a presentation of experimental data demonstrating the performance by baseline measurements as well as thermogravimetric measurements on $Fe_{78}Cr_{22}$ steel in air and in humidified air (90% water vapour). The novel equipment reveals a good temperature stability demonstrated by isothermal baseline measurements. A significant difference in corrosion between dry and humidified atmosphere is shown and the corrosion mechanisms in humidified atmosphere is discussed.

Experimental

Instrument design

A schematic of the set-up is shown in Fig. 1. The basic unit is a STA409PG-Luxx with an electronic balance where, the standard furnace has been exchanged with the newly developed water vapour furnace. A water vapour generator system was also developed for the system.

The reactive gas system comprises of a liquid water flow controller that supplies water to an evaporator. The water is supplied from a water bottle by applying a small overpressure (0.5 mbar) in the bottle (Fig. 1). Another gas may be mixed with the water vapour inside the evaporator, so that the analysis is performed in a gas constituting 0–100% water vapour. The humidified reactive gas is subsequently fed to the water vapour furnace chamber through a heated gas transfer line. The protective gas for the balance is supplied directly into the balance chamber.

A cross section of the water vapour furnace, sample holder and balance protective alumina tube is given in Fig. 2. The heating elements are shielded by the outer protective alumina tube. The humidified at-

* Author for correspondence: mette.solvang@risoe.dk

1388–6150/$20.00

Akadémiai Kiadó, Budapest, Hungary
Springer, Dordrecht, The Netherlands

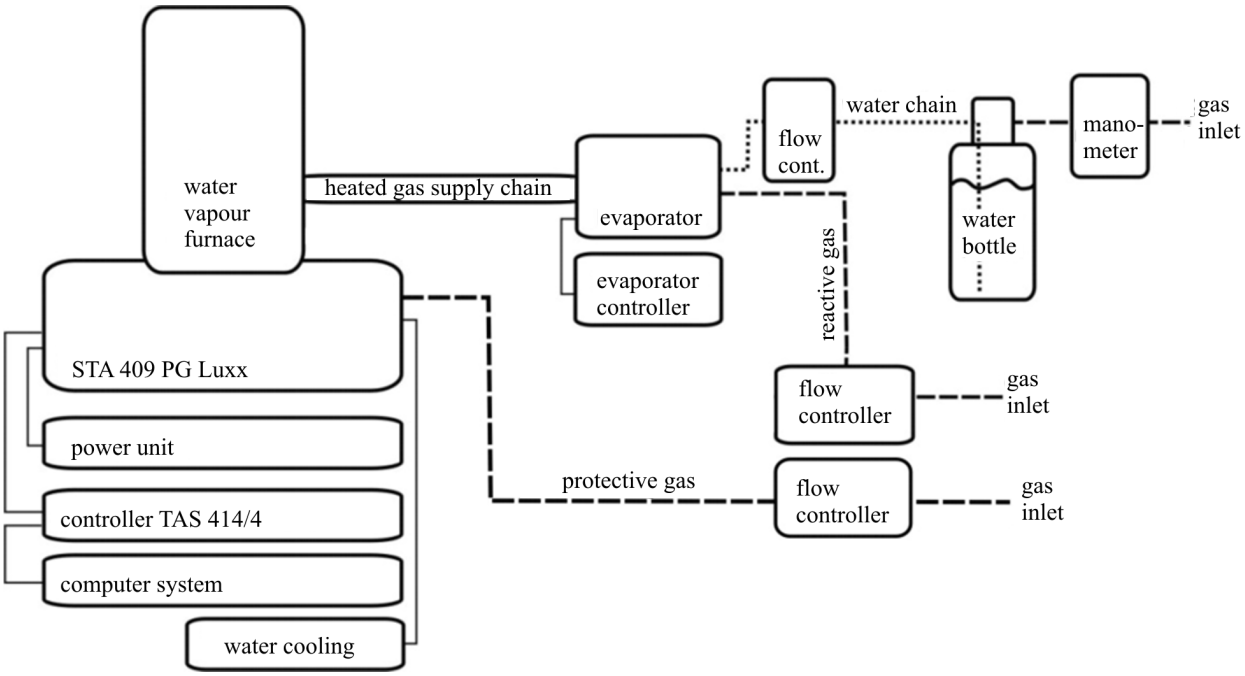

Fig. 1 The high temperature thermogravimetric set-up for measuring in a humidified atmosphere

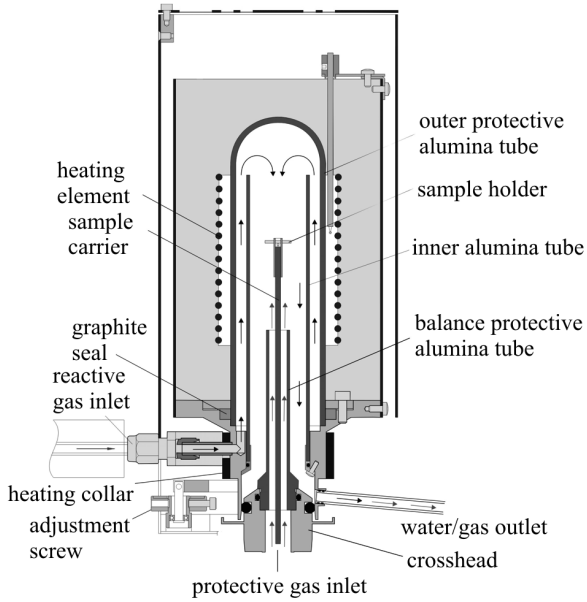

Fig. 2 A cross section of the furnace, sample carrier system and sample holder. The flow pattern of the gases is shown. The sketch is not to scale

mosphere enters the furnace via a tube with a heating collar and is directed to the top of the furnace by an inner alumina tube as indicated in Fig. 2. At the top of the furnace the reactive gas is forced downwards inside the inner alumina tube and passes the sample. The protective gas from the balance chamber passes through the balance protective alumina tube, which is placed on to the crosshead. The reactive gas and the protective gas are mixed above the balance protective alumina tube but below the sample, and the gases leave the system at the base of the furnace.

The operation of the equipment is similar to the operation of standard thermogravimetric equipments. The furnace temperature must, however, exceed 150°C before water vapour is fed through the system in order to avoid condensation. Gases, for example N_2, Ar, Ar/H_2 (7% H_2) and N_2/H_2 (9% H_2) have been used along with the water vapour as both the reactive and protective gases. The recommended flow rate for both gases was found to be 20–50 mL min^{-1}.

The stability of the instrument was tested under different conditions. The long-term isothermal stability was tested at 900°C for 16 h in 50% humidity and 50% air (Table 1). The effect of varying the water vapour content was examined through an isothermal test at 800°C for 72 h. The water vapour content was changed in steps of 0–50–90% water vapour with a hold time of 24 h for each. The test conditions are summarised in Table 1.

Thermogravimetric measurements

The measurements were performed on a $Fe_{78}Cr_{22}$ steel to examine the oxidation behaviour in dry and humidified air. Specimens of a 200 μm thick foil were cut with the dimensions 10×20 and 18×20 mm^2. A hole was drilled in the foils enabling up to four specimens to be suspended freely in each measurement. Isothermal measurements were performed at 1100°C in air and in humidified air for 48 h. In addition, measurements were

Table 1 The measurement conditions for the thermogravimetric baseline runs (B1–B4) and experiments S1–S4 on $Fe_{78}Cr_{22}$ steel plates

	Heating/K min^{-1}	Cooling/K min^{-1}	Isotherm/h	T_{max}/°C	Reactive gas/mL min^{-1}		Protective gas/mL min^{-1}
					H_2O	air	air
baselines							
B1	40	–	16	900	30	30	30
B2	10	10	24	800	–	40	40
B3	10	10	24	800	20	20	40
B4	10	10	24	800	36	4	40
1. series							
S1	10	10	48	1100	–	40	40
S2	10	10	48	1100	36	4	40
2. series							
S3	0.5	10	–	1250	–	40	40
S4	0.5	10	–	1250	36	4	40

performed in dry and humidified air as temperature scans from room temperature to 1250°C at a heating rate of 0.5 K min^{-1}. The measurements were corrected for buoyancy utilising platinum foils as inert samples. Table 1 summarises the measurement conditions.

Polished cross sections of the specimens were prepared for examination. The microstructure of the cross sections was evaluated using scanning electron microscopy (SEM, JEOL, JSM 5310) equipped with an energy dispersive X-ray (EDX) analyser.

Results and discussion

Instrument stability

Figure 3 shows the mass signal of the isothermal baseline B1 as a function of time. The mass signal shows only slight fluctuations over a period of 16 h. The temperature of the laboratory was recorded during testing, and a day and night fluctuation of less than 1°C was found. However, the observed stability can only be achieved under stable laboratory temperatures (T_{lab}), as discussed in the following.

Isothermal baselines (B2–B4) are shown in Fig. 4 as a function of time. The measurements were conducted using three different atmospheres in 24 h as indicated in Fig. 4 (Table 1). T_{lab} was recorded during testing, and a day and night fluctuation of approx. 4°C was found. The oscillation of the mass signal in Fig. 4 correlated with fluctuation in the T_{lab}. Consequently, the mass signal was not influenced by changes of the reactive gas atmosphere, and eventually no condensation of water vapour was observed during the measurements performed in the humidified atmosphere. Thus, a good stability of the baseline was documented also when the atmosphere was humidified. A stable T_{lab} is, however, critical for high stability of the thermogravimetric signal.

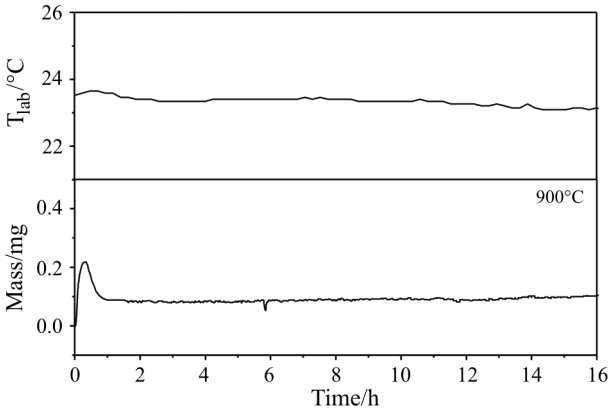

Fig. 3 The isothermal baseline run at 900°C (B1) and the laboratory temperature as a function of time. Air was used as the reactive and protective gases

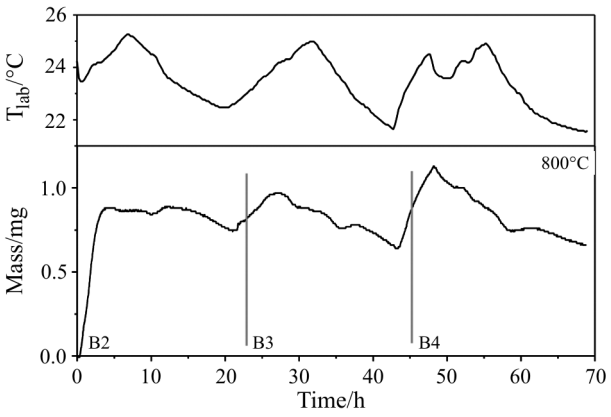

Fig. 4 The isothermal baseline run at 800°C; B2 – 100% air/0% H_2O, B3 – 50% air/50% H_2O, B4 – 10% air/90% H_2O; and the laboratory temperature as a function of time. The reactive gas was changed in steps during the test (Table 1)

Thermogravimetric measurements on $Fe_{78}Cr_{22}$

Figure 5 shows the mass gains as a function of time for specimens S1 and S2. It is evident that the specimen exposed to humidified air exhibits a much larger mass gain than the corresponding specimen exposed to dry air (i.e. 62 and 11 mg cm^{-2}, respectively). Micrographs of the polished cross section are shown in Fig. 6 for the two specimens. The difference in scaling should be noticed; specimen S2 is thicker than specimen S1. The difference in mass gain between the two specimens is also reflected in the microstructure. Specimen S1 (Fig. 6a) has grown a 10–15 μm thick oxide scale. The composition of the scale was identified as a thick inner layer of Cr_2O_3 (chromia) and a thin outer layer of iron–chromium oxide. Specimen S2 was oxidised all through the specimen (Fig. 6b), and the heat-treated specimen was 350–500 μm thick as compared to 200 μm before the oxidation. The center of the specimen consists of a porous iron–chromium oxide layer, while the outer 40–80 μm consists of a dense iron-oxide layer. A small chromium-enriched layer can be identified between the two regions (Fig. 6). The three different regions can be distinguished from the contrast difference in the micrograph. Figure 7 shows the mass gain as a function of temperature for specimen S3 and S4. The oxidation rate increases slowly for specimen S3 at ca. 1150°C, while the oxidation rate for specimen S4 increases rapidly at ca. 1100°C. The mass gain is largest for the specimen oxidised in humidified air relative to dry air (56 *vs*. 5 mg cm^{-2}). The microstructures of specimens S3 and S4 are shown in Fig. 8. The compositions and microstructures of the specimens are similar to the microstructures described previously for specimens S1 and S2 (cf. Figs 6 and 8).

The large difference in mass gain is attributed to the presence of water vapour. Before discussing the dramatic effect of water vapour, the oxidation behaviour of chromia forming iron–chromium alloys will be described in order to understand the large differences in the developed microstructures. During the initial oxidation, a continuous layer of chromia is formed at the surface of the alloy, and further oxidation of the alloy is governed by a steady state growth of a chromia scale. The steady state oxidation is characterised by a slow growing chromia scale, which is governed by the transport of reactants in the grain boundaries of the chromia scale. Due to the build up of compressive growth stresses in the scale during the oxidation, the chromia scale may eventually crack [4]. If the cracks extend through the oxide scale, the alloy surface will be exposed to oxidants. The alloy surface becomes depleted in chromium as a result of the oxidation, so the freshly exposed alloy surface has a decreased content of chromium relative to the original content. If a sufficient amount of chromium is present (ca. 15 at%) at the alloy surface, the chromia scale will reform [5, 6]. Otherwise, the formation of iron rich oxides starts at the alloy surface. Iron rich oxides grow faster than chromia, so a fast oxidation process is initiated where an iron oxide is formed on top of the pristine chromia layer and a porous iron–chromium oxide is formed beneath the pristine chromia layer, a so-called breakaway oxidation [7].

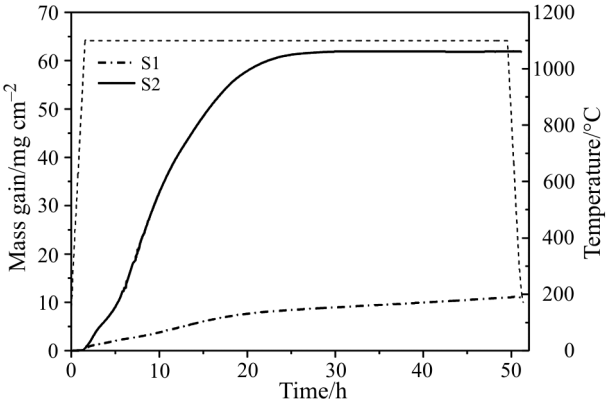

Fig. 5 The mass gain as a function of time for specimens S1 and S2 at isothermal oxidation at 1100°C. The heat-treatment was carried out in a dry and a humidified atmosphere. The temperature profile is also shown

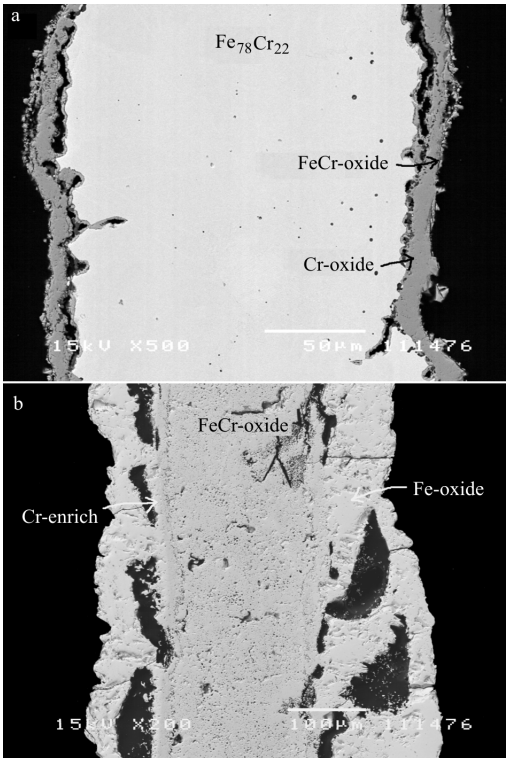

Fig. 6 SEM micrograph of the scale grown for 48 h at 1100°C; a – specimen S1, b – specimen S2, note that the two micrographs have different magnification

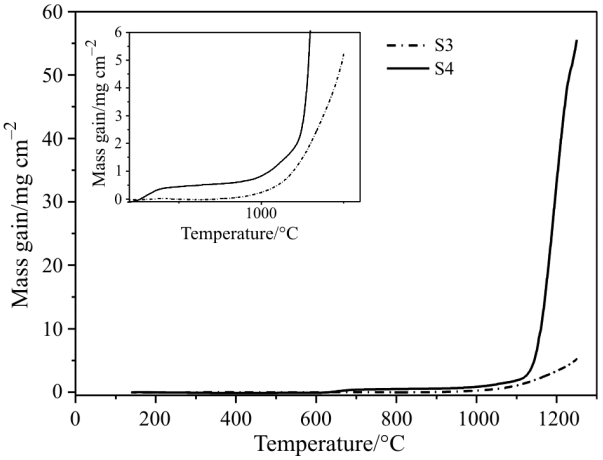

Fig. 7 The mass gain as a function of temperature for specimens S3 and S4. The heat-treatment was carried out in dry and in humidified atmospheres

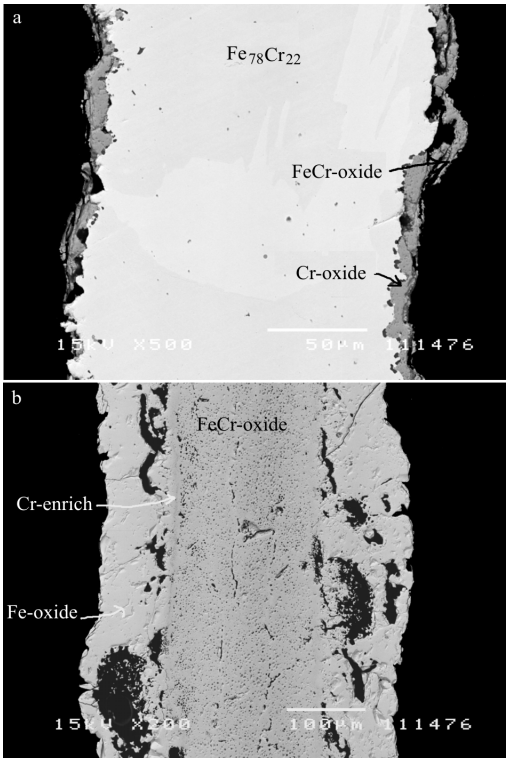

Fig. 8 SEM micrograph of the scale grown under a temperature scan between room temperature and 1250°C at a heating rate of 0.5 K min^{-1}; a – specimen S3, b – specimen S4, note that the two micrographs have different magnification

The formation of iron-rich oxides for the specimens exposed to humidified air is a result of breakaway oxidation. The breakaway oxidation is also clearly seen from the thermogravimetric curves, where the rapid increase in mass indicates the initiation of breakaway oxidation (Figs 5 and 7). The specimens exposed to dry air formed a dense layer of chromia with a small amount of iron–chromium oxide as the outermost oxide (Figs 6a and 8a). The presence of iron-oxide indicates that cracks formed during the oxidation. In contrast to the specimens grown in humidified air, however, the chromia scale reformed in this case.

How can the detrimental effect of water vapour on the oxidation process be explained? Breakaway oxidation is initiated by cracks in the protective chromia scale, so the presence of water vapour must increase the tendency of crack formation. The effect of humidity may be attributed to the formation of thicker scales, since cracks in general form easier in thick oxide scales [8]. The presence of water vapour can also alter the mechanical properties of the scale. These two effects will be discussed in the following.

The parabolic growth rate of chromia scales increases when the reactive atmosphere (air or oxygen) is humidified [9]. The reason for this is unclear. Hydrogen can dissolve as protons in chromia, where they bond to oxygen to form hydroxide ions in the oxide [10]. This may alter the defect concentration of the rate determining species. It has been shown that the rate determining defect species is chromium interstitials, while oxygen vacancies are the minority defects during the growth of chromia [11]. Proton defects have a relatively positive charge, so the dissolution will result in a decrease of chromium interstitials and oxygen vacancies according to the electroneutrality principle, so this cannot explain an increased growth rate. Another explanation is an increased mobility of defects in the oxide. The ionic radius of hydroxide ions is considerably smaller than the corresponding radius for oxide ions (0.095 *vs*. 0.140 nm) [12]. This leads to an increased mobility in the scale and thereby an increased growth of the chromia scale. The most probable cause for the increase in oxidation rate after the addition of water vapour appears thus to be the greater mobility of oxygen ions by way of hydroxide ions, or an increased formation of high diffusivity paths as described below. However, further experimental evidence is needed for verification.

Alternatively, the mechanical properties of the chromia scale may change after the dissolution of hydrogen in chromia. The stresses generated during the growth of chromia scales are relieved through plastic deformation of the oxide. The plastic deformation of scales is limited by the minority defect in the scale [10], which for chromia scale are oxygen vacancies. So the plastic deformation of chromia scales is limited by oxygen vacancies. The dissolution of protons in the oxide decreases the content of oxygen vacancies, as previously mentioned. Thus, the presence of water vapour may decrease the ability of the chromia scale to deform

plastically. The generation of growth stresses may therefore lead to an increased formation of high diffusivity paths in the scale. The formation of high diffusivity paths in the scale increases the growth rate of the scale, and may result in breakaway oxidation in cases where a crack propagates through the chromia scale. Another effect of hydrogen could be that hydrogen dissolves in the alloy matrix, when protons diffuse inward through the chromia scale. This may result in brittleness in the alloy, and subsequently loss of chromia adhesion to the alloy and thereby initiation of breakaway oxidation [9].

Although the growth of chromia increases as a result of water vapour, the increase in growth rate is not dramatic [9]. The change in mechanical properties of the chromia scale after the dissolution of protons is therefore believed to be the most important effect for the detrimental effect of water vapour on the oxidation behaviour.

Conclusions

An instrument for high temperature thermogravimetric measurements in a humidified atmosphere was successfully designed. The instrument is a re-design of the existing commercial instrument: STA409PG-Luxx, Netzsch to which a new furnace, a new sample carrier system, sample holder, a supply system for the humidified atmosphere, an evaporator and water flow controller were developed.

The instrument was tested and found suitable for measuring in a humidified air. The baseline measurements showed small drift although a scatter in the mass signal was detected. This scatter was, however, mainly caused by the change of temperature in the laboratory.

Heat-treatment of $Fe_{78}Cr_{22}$ steel plates using either dry or humidified air demonstrated a pronounced difference in the mass gain as a function of atmosphere, temperature and time. The specimens exposed to humidified air exhibited a breakaway oxidation, while the specimens oxidised in dry air formed a dense chromia scale. This detrimental effect of water vapour is most likely caused by a change in mechanical properties of the protective chromia scale.

Acknowledgements

We would like to thank Bo Holdt Simonsen for technical assistance and Helmer Nilsson for specimen preparation.

References

1 L. Mikkelsen, P. H. Larsen and S. Linderoth, J. Therm. Anal. Cal., 64 (2001) 879.
2 N. Q. Minh, Science and Technology of Ceramic Fuel Cells, Elsevier, Amsterdam 1995, p. 366.
3 H. J. Grabke, in: H. J. Grabke, D. B. Meadowcroft (Eds), Guidelines for Methods of Testing and Research in High Temperature Corrosion, Institute of Materials, London 1995, p. 52.
4 H. E. Evans, Int. Mater. Rev., 40 (1995) 1.
5 F. Gesmundo and Y. Niu, Oxid. Met., 50 (1998) 1.
6 F. Gesmundo and F. Viani, Oxid. Met., 25 (1986) 269.
7 H. E. Evans, A. T. Donaldson and T. C. Gilmour, Oxid. Met., 52 (1999) 379.
8 A. Rahmel and M. Schutze, Oxid. Met., 38 (1992) 255.
9 P. Kofstad, High Temperature Corrosion, Elsevier, London 1988, p. 385.
10 T. Norby, J. Phys. IV, 3 (1993) 99.
11 L. Mikkelsen and S. Linderoth, Mater. Sci. Eng. A, 361 (2003) 198.
12 H. Nickel, Y. Wouters, M. Thiele and W. J. Quadakkers, Fresenius J. Anal. Chem., 361 (1998) 540.